Transactions of the Korean Nuclear Society Autumn Meeting
Changwon, Korea, October 24-25, 2024

Evaluation Method and Comparison of Correlations for the Thermal Creep of manufactured HT9 Cladding

Dong-Ha Kim [a, b], Sunghwan Yeo [a*], Jun-Hwan Kim [a], Sung-Ho Kim [a], Jeong-Mok Oh [a], Cheol-Min Lee [a], Yong-Kook Lee [b, c]

[a]*Korea Atomic Energy Research Institute, 989-111 Daedeok-daero, Yuseong-gu, Daejeon 34057, Korea*
[b]*Department of Materials Science and Engineering, Yonsei University, 50, Yonsei-ro, Seoul 03722, Korea*
[c] *Graduate Institute of Ferrous & Eco Materials Technology, Pohang University of Science and Technology, Pohang, 37673, Republic of Korea*

*Corresponding author: syeo@kaeri.re.kr

Keywords : ferritic/martenstic steel, 12Cr1MoV, HT9, thermal creep, correlation

1. Introduction

9—12%Cr Ferritic Martensitic Steel (FMS), such as HT9, possess excellent high-temperature strength and corrosion resistance suitable for use in turbines and boilers for fossil-fired, coal, and gas power plants [1-3]. FMS also exhibit higher thermal conductivity and excellent void swelling resistance under neutron irradiation compared to those of austenitic steel leading to a candidate material for nuclear fuel cladding in Sodium-cooled Fast Reactor (SFR) and Small Modular Reactors (SMRs). Over the past few decades, the selection of cladding materials has been performed. HT9, in particular, was tested as a nuclear fuel cladding material in the experimental reactors such as Experimental Breeder Reactor-II (EBR-II) and Fast Flus Test Facility (FFTF) in the United States during the 1970s, with irradiation levels reaching up to 200 dpa [4].

The creep resistance of nuclear fuel cladding is a key factor determining the mechanical strength and life-limiting of fuel rod. In this study, the thermal creep strain for HT9 cladding composed primarily of 12% Cr and 1% Mo, produced by the Korea Atomic Energy Research Institute (KAERI). The thermal creep tests were conducted for up to 20,000-h. These data were compared with that of publications and correlation models. Rather than comparing the performance of the developed fuel claddings, the objective is to validate the mechanical performance of manufactured HT9.

2. Methods and Results

The HT9 ingot was manufactured by SeAH Special Steel Co., Ltd. through a vacuum induction melting (VIM) and electro-slag re-melting (ESR) process. The produced ingot was heated and hot-forged at 1170 ℃, followed by processing into a round bar with a diameter of 160 mm. After hot extrusion at 1170 ℃, cold drawing, intermediate heat-treatment, and cold pilering were performed to produce a mother tube with an outer diameter of 19.05 mm and a thickness of 1.24 mm. The mother tube was then transferred to Iljin Steel co., Ltd., where it underwent four cycles of clod drawing and intermediate heat-treatment to manufacture HT9 cladding with an outer diameter of 7.4 mm and a thickness of 0.56 mm. The chemical composition of the manufactured HT9 cladding is shown in Table 1. The final heat-treatment conditions were normalizing at 1038 ℃ for 6 minutes and tempering at 760 ℃ for 40 minutes

Table 1. The chemical elements of manufactured HT9 cladding in wt.%.

Element	**Fe**	**C**	**Si**	**Mn**	**Ni**	**Cr**	**Mo**
Wt.%	**Bal.**	**0.18**	**0.2**	**0.59**	**0.59**	**11.99**	**1.00**
Standard deviations	**Bal.**	**±0.01**	**±0.05**	**±0.05**	**±0.05**	**±0.2**	**±0.05**
Element	**W**	**V**	**Nb**	**Al**	**P**	**S**	
Wt.%	**0.54**	**0.30**	**0.008**	**0.01**	**0.005**	**0.003**	
Standard deviations	**±0.2**	**±0.05**					

2.1 Thermal creep test and measurement method

The specimens used for the thermal creep test were prepared by cutting the manufactured HT9 cladding into 47 mm lengths and arc welding both ends with HT9 end caps. A gas channel was designed in one of the end caps to allow for pressure injection, and pressure was applied using a pressurization welding system according to the test stress. The prepared thermal creep specimens were sealed in a quartz with tantalum foil to prevent oxidation and then laded into a furnace set to the test temperature. After lading, the specimens were removed from the furnace every 1,000 hours, and the diameter was measured using a laser diameter measurement system at

5 mm intervals of thermal creep specimen, excluding the welded areas. And the thermal creep specimen was rotated 90 degrees for a total of four diameter measurements. Detailed information on the thermal creep strain measurement has been previously reported in a prior study [5].

The thermal creep test was conducted under the effective stress ranging from 9 to 102 MPa, and the temperature ranging from 600 to 650 °C, considering the operating environments of the generation IV reactors, specifically the Sodium-cooled Fast Reactor (SFR) and the globally developed Small Modular Reactors (SMRs), as well as the need to enhance reactor efficiency. To achieve high efficiency in these reactors. Fig. 1 shows the creep strain curves up to 20,000-h obtained from the thermal creep test.

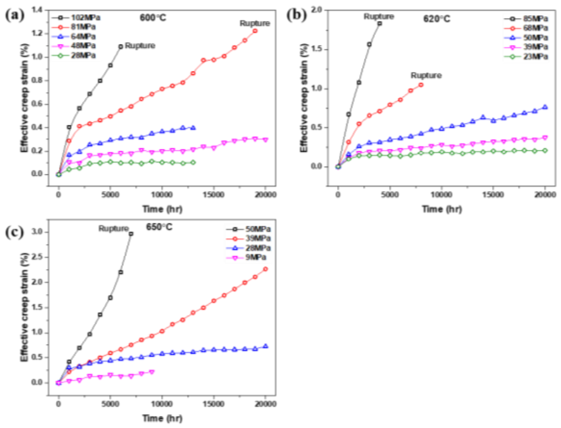

Figure 1. The obtained thermal creep strain curves of manufactured HT9 cladding in effective stress ranges of 9—102MPan at (a) 600℃, (b) 620℃, and (c) 650℃

2.2 Thermal creep strain and correlations

There are available thermal creep strain data and correlations of HT9 in the literatures. First, the theta projection concept, developed by Evans [6], uses the theta function to mathematically evaluate creep behavior. Lewis and Chuang [7] proposed the theta projection method (TPM) for HT9 thermal creep. The theta projection method is given by the following equation:

$$\varepsilon_T = \theta_1\left(1 - e^{-\theta_2 t}\right) + \theta_3\left(e^{\theta_4 t} - 1\right) \quad (1)$$

where ε_T is the total creep strain, θ_1 and θ_3 are scaling parameters for describing the primary and tertiary stages with respect to a strain. θ_2 and θ_4 are rate parameters for characterizing the curvatures of the primary and tertiary stages. t is absolutely time in sec. Each θ value is expressed as a function of stress and temperature.

$$\log \theta_i = a_i + b_i\sigma + c_i T + d_i\sigma T \quad (2)$$

where a_i, b_i, c_i, and, d_i are the coefficients. σ is the tress in MPa. T is the temperature in K.

The second thermal creep correlation to be compared is the modified Garofalo's equation [8], which utilizes the power law [9], Arrhenius equation [10], and Garofalo's equation [11]. This correlation was developed based on thermal creep data obtained from experiments conducted by Briggs et al [8].

$$\bar{\varepsilon}_T = \bar{\varepsilon}_{TP} + \bar{\varepsilon}_{TS} + \bar{\varepsilon}_{TT} \quad (3)$$

$$\bar{\varepsilon}_{TP} = \left[C_1\, exp\left(\frac{-Q_1}{RT}\right)\bar{\sigma} + C_2\, exp\left(\frac{-Q_2}{RT}\right)\bar{\sigma}^4 + C_3\, exp\left(\frac{-Q_3}{RT}\right)\bar{\sigma}^{0.5}\right]\cdot\left(1 - exp[-C_4 t]\right) \quad (4)$$

$$\bar{\varepsilon}_{TS} = \left[C_5\, exp\left(\frac{-Q_4}{RT}\right)\bar{\sigma}^2 + C_6\, exp\left(\frac{-Q_5}{RT}\right)\bar{\sigma}^5\right]\cdot t \quad (5)$$

$$\bar{\varepsilon}_{TT} = C_7\, exp\left(\frac{-Q_6}{RT}\right)\bar{\sigma}^{10}\bar{t}^4 \quad (6)$$

where $\bar{\varepsilon}_T$, $\bar{\varepsilon}_{TP}$, $\bar{\varepsilon}_{TS}$, and, $\bar{\varepsilon}_{TT}$ are total, primary, secondary, and tertiary creep. *C, Q, R, T, t,* and, $\bar{\sigma}$are material constant, activation energy, gas constant, temperature K, time s, and effective stress MPa.

2.3 Comparison between thermal creep data and correlations

The thermal creep data for HT9 cladding obtained by Toloczko et al [12], Sandvik Steel [13], and from this study conducted at KAERI were compared based on the TPM [7] and modified Garofalo's equation (MGE) [ref]. In Fig. 2, the thermal creep data were primarily compared at 600 °C, as this was the common temperature across the studies. However, for the Sandvik data [13], creep strain curve at three different temperatures were presented since only on stress data was available at each temperature. The dashed lines represent the TPM, while the solid lines represent the MGE. The KAERI thermal creep strain curves in Fig. 2(c) predominantly exhibit secondary creep strain, so the equations were applied only to primary and secondary creep. Among the three thermal creep datasets in Fig. 2, only the Sandvik [13] creep data in Fig. 2(b) match well with the TPM. The other thermal creep data and correlations do not match well, particularly in the transition from primary to secondary creep, and in the creep strain behavior. Although the KAERI thermal creep strain curves in Fig 2(c) appears similar to the MGE [8], the differing stress levels indicate that this match is also not accurate.

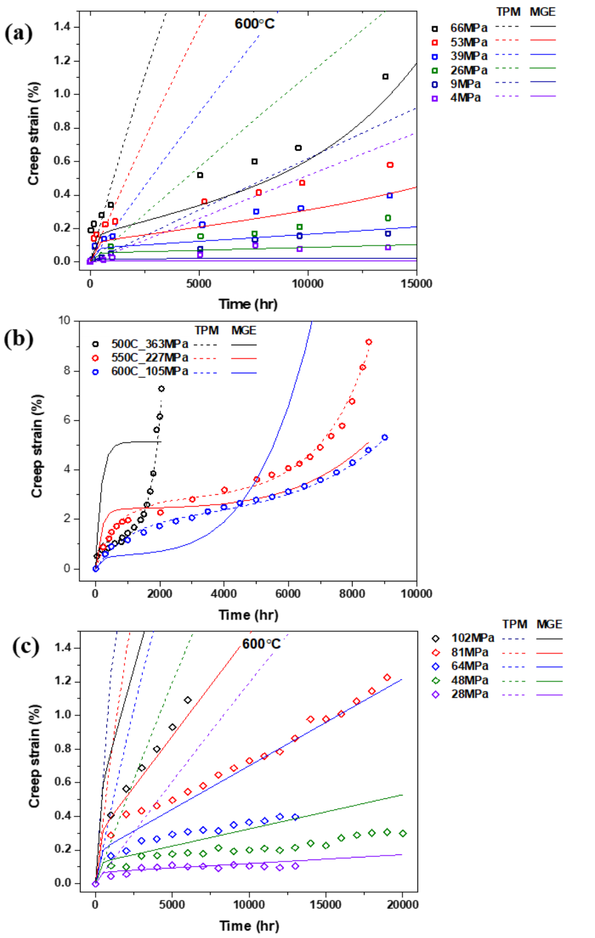

Figure 2. Comparison graphs of thermal creep strain curves and correlations (a) Toloczko et al [12] data at 600 ℃, (b) Sandvik Steel [13] data at 500 ℃, 550 ℃, and 600 ℃, and (c) experimentally obtained thermal creep data (KAERI) at 600 ℃.

2.4 Steady-state creep rate

The behavior and life-time of thermal creep, as well as the mechanisms of creep strengthening, could be evaluated through the secondary creep rate. Since the experimentally obtained data in this study exhibit secondary creep in the thermal creep strain curves, the secondary creep rates were compared. The TPM was excluded from the comparison because it was developed based on the behavior of primary and tertiary creep. Instead, the creep rates were compared with those predicted by the MGE [8]. Fig. 3 shows a log-scale graph of the effective strain rate versus effective stress in the 600—650 ℃ range. The MGE utilized the creep rate equation shown in Equation (5). The experimentally obtained creep rates were determined by selecting the linear regime of the thermal creep strain curve and calculating the slope.

The increasing creep rate with increasing stress shows the same trend in both the experimentally obtained data and the MGE [8]. However, differences in the rate of increase and the absolute rate values were observed across the stress rages. These differences in slope indicate variation in the creep strengthening mechanisms [14].

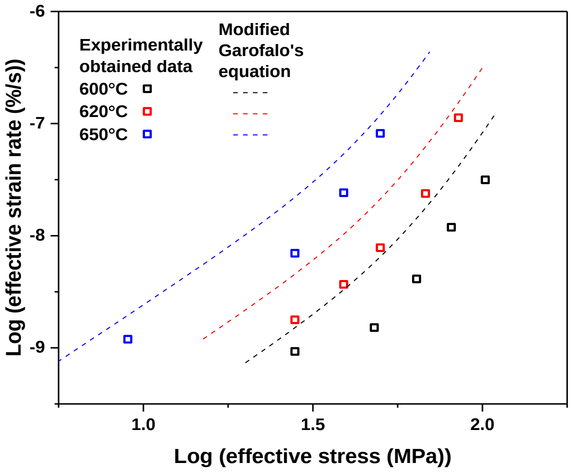

Figure 3. Log-scale effective strain rate versus of experimentally obtained dada and modified Garofalo's equation [8] in the 600—650 ℃ range

3. Conclusions

This study evaluated the thermal creep properties of HT9 cladding developed by the Korea Atomic Energy Research Institute (KAERI). HT9 cladding, a 9—12% Cr Ferritic Martensitic Steel (FMS) with excellent high-temperature strength and corrosion resistance, is a promising candidate for nuclear fuel cladding in Sodium-cooled Fast Reactor (SFR) and small modular reactors (SMRs). The study assessed thermal creep behavior based on thermal creep experimental data, focusing on the correlation between creep rate and stress within the temperature range of 600—650 ℃.

In this process, the experimental data were analyzed using the Theta Projection Method (TPM) and modified Garofalo's equation (MGE), and differences in thermal creep behavior were identified through comparisons with existing literature. The MGE, which includes creep strengthening mechanisms, provided a physically meaningful relationship and demonstrated behavior similar to the experimentally obtained data. However, differences in the slope between the experimental data and the correlation indicated variations in the creep strengthening mechanisms. This suggests the need to recalibrate existing thermal creep correlation or develop new one.

In conclusion, this study validated the mechanical performance of HT9 cladding and contributed to providing essential baseline data for the safe and reliable operation of nuclear reactors.

REFERENCES

[1] L. Egnell, N. Persson, On the creep properties of Sandvik HT7 and HT9, Ferritic steels for fast reactor steam generators. Proceedings of an international conference held by the British Nuclear Energy Society at the Institution of Civil Engineers, London 30 May-2 June 1977, 1978.

[2] V.K. Sikka, Ferritic alloys for use in nuclear energy technologies, TMS-AIME, Warrendale, PA (1984) 317-27.

[3] R. Klueh, A.T. Nelson, Ferritic/martensitic steels for next-generation reactors, J. Nucl. Mater. 371(1-3) (2007) 37-52.

[4] D. E. Burkes, R. S. Fielding, D. L. Porter, D. C. Crawford, and M. K. Meyer, A US perspective on fast reactor fuel fabrication technology and experience part1: metal fuels and assembly design, J. Nucl. Mater. 389, 458 (2009).

[5] D. H. Kim, C. M. Lee, J. H. Kim, S. H. Kim, S. H. Yeo, Y. K. Lee, Thermal Creep Analysis and Correlation Development for Manufactured HT9 cladding, J. Nucl. Mater 593 (2024) 154999.

[6] R. Evans, J. Parker, B. Wilshire, The θ projection concept—A model-based approach to design and life extension of engineering plant, International Journal of Pressure Vessel and Piping, Vol. 50, p. 147, 1992.

[7] G. Lewis, C.-C. Chuang, Constitutive thermal creep deformation relations for lifetime prediction of a fusion reactor first wall ferritic alloy, Fusion Engineering Design, Vol. 13, p.407, 1991.

[8] L.L. Briggs, Y.I. Chang, D. Hill, J. Ahrens, M. Billone, D. Crawford, E. Filewicz, P. Finck, E. Fujita, K. Grimm, Safety Analysis and Technical Basis for Establing an Interim Burnup Limit for Mark-V and Mark-VA Fuel Subassemblies in EBR-II, Argonne National Lab.(ANL), Argonne, ILUnited States, 2018.

[9] F.H. Norton, The creep of steel at high temperatures, McGraw-Hill, New York (1929).

[10] X. Niu, L. Shen, C. Chen, J. Zhou, L. Chen, An Arrhenius-type constitutive model to predict the deformation behavior of Sn0. 3Ag0. 7Cu under different temperature, J. Mater. Sci: Mater. Electron. 30 (2019) 14611-14620.

[11] F. Garofalo, D.B. Butrymowicz, Fundamentals of creep and creep-rupture in metals, Macmillan, New York, 1965.

[12] M. Toloczko, B. Grambau, F. Garner, K. Abe, Comparison of Thermal Creep and Irradiation Creep of HT9 Pressurized Tubes at Test Temperatures from ~ 490° C to 605° C, Effects of Radiation on Materials: 20th International Symposium, ASTM International, 2001.

[13] L. Egnell, N. Persson, On the creep properties of Sandvik HT7 and HT9, Ferritic steels for fast reactor steam generators. Proceedings of an international conference held by the British Nuclear Energy Society at the Institution of Civil Engineers, London 30 May-2 June 1977, 1978.

[14] L. Kolc, V. Sklenicka, A. Dlouhy, K. Jucharova, in: A. Strang, J. Cawley, G.W.Greenwood (Eds.), Microstructural stability of creep resistant alloys for high temperature plant applications, vol. 445–455, IOM, London, 1998.